Morphological and chemical evaluation of bone with apatite-coated Al_2O_3 implants as scaffolds for bone repair

(Avaliação morfológica e química do osso com implantes de Al_2O_3 recobertos com apatita como suporte para a reparação óssea)

A. L. M. Maia F.[1,3], J. L. da Silva[1,2], F. P. M. do Amaral[1], A. A. Martin[3], A. O. Lobo[4], L. E. S. Soares[3]

[1]Laboratório de Fisiologia da Faculdade Diferencial, Facid e Faculdade Santo Agostinho, FSA, Teresina, PI, Brasil.

[2]Laboratório de Anatomia da Faculdade Diferencial, Facid Teresina, PI ,Brasil

[3]Laboratory of Biomedical Vibrational Spectroscopy -LEVB, [4]Laboratory of Biomedical Nanotechnology - NANOBIO, Research and Development Institute - IP&D, UNIVAP, Av. Shishima Hifumi 2911, Urbanova, S. José dos Campos, S. Paulo, Brazil 12244-000

almmaiaf@ig.com.br, jucelinolopes@uol.com.br, fabricio27amaral@yahoo.com.br, amartin@univap.br, aolobo@univap.br, lesoares@univap.br

Abstract

The clinical challenge in the reconstruction of bone defects has stimulated several studies in search of alternatives to repair these defects. The ceramics are considered as synthetic scaffolds and are used in dentistry and orthopedics. This study aimed to evaluate by micro energy-dispersive X-ray fluorescence spectrometry (μ-EDXRF) and scanning electron microscopy-energy dispersive spectroscopy (SEM-EDS), the influence of uncoated and apatite-coated Al_2O_3 implants on bone regeneration. Twelve samples of Al_2O_3 implants were prepared and half of this samples (n = 6) were apatite-coated by the modified biomimetic method and then the ceramic material were implanted in the tibia of rabbits. Three experimental groups were tested: Group C – control, surgery procedure without ceramic implant, Group Ce – uncoated Al_2O_3 implants (n = 6) and Group CeHA - apatite-coated Al_2O_3 implants (n = 6). The deposition of bone tissue was determined by measuring the weight content of Ca and P through surface mapping of bone-implant interface by μ-EDXRF and through point analysis by EDS. It was observed after thirty days of treatment a greater deposition of Ca and P in the group treated with CeHA ($p < 0.001$) compared to group C. The results suggest that ceramic coated with hydroxyapatite (CeHA) can be an auxiliary to bone deposition in tibia defect model in rabbits.

Keywords: ceramic implants, bone, X-ray spectrometry, microscopy.

Resumo

O desafio clínico na reconstrução de defeitos ósseos tem estimulado vários estudos em busca de alternativas para reparar esses defeitos. As cerâmicas são consideradas como suportes sintéticos e são utilizadas em odontologia e ortopedia. Este estudo teve como objetivo avaliar por micro fluorescência de raios X por energia dispersiva (μ-EDXRF) e microscopia eletrônica de varredura-espectroscopia de dispersão de energia (MEV-EDS), a influência dos implantes de Al_2O_3 sem recobrimento e recobertos com apatita, na regeneração óssea. Doze amostras de implantes de Al_2O_3 foram preparadas e metade destas amostras (n = 6) foi revestida com apatita pelo método biomimético modificado e em seguida o material cerâmico foi implantado na tíbia de coelhos. Três grupos experimentais foram testados: Grupo C - controle, procedimento cirúrgico sem implante de cerâmica, Grupo Ce - implantes de Al_2O_3 sem recobrimento (n = 6) e Grupo CeHA - implantes de Al_2O_3 recobertos com apatita (n = 6). A deposição de tecido ósseo foi determinada através da medição do teor em peso de Ca e P na interface osso-implante através de mapeamento de superfície por μ EDXRF e através da análise pontual por EDS. Observou-se depois de 30 dias de tratamento, uma maior deposição de Ca e P para o grupo tratado com CeHA ($p < 0,001$) em comparação ao grupo C. Os resultados sugerem que a cerâmica recoberta com hidroxiapatita (CeHA) pode ser um auxiliar de deposição óssea no modelo de defeito tibial em coelhos.

***Palavras-chave**: implantes cerâmicos, osso, espectrometria de raios X, microscopia.*

INTRODUCTION

Biomaterials are temporary matrices for bone growth by providing specific environment architecture for the development of tissue. They also can be used as a vehicle for drugs delivery such as antibiotics and chemotherapeutic agents and even as scaffolds for the growth factors [1]. Porous bioceramics are widely used in medical applications such as bone substitutes or bone filling material [2].

Tissue Engineering is a new field of biotechnology

that focuses on developing biological equivalents in order to repair or replace damage tissues [3, 4]. The clinical challenge in the reconstruction of bone defects has stimulated several studies to repair these defects. These studies include autografts, allografts and tissue engineering [5]. In autografts the tissue from the patient is used to reconstruct defects at a distant location, occurring complications as infections [6]. A key component in tissue engineering for bone regeneration is the scaffold that acts as a template for cell interactions and the formation of bone-extracellular matrix that provides mechanical support to the newly formed tissue [7]. Among the new materials used to act as scaffolds the ceramics based on alumina (Al_2O_3) and zirconia (ZrO_2) are highlighted [8].

In recent years, it was discovered the complexity of the mechanisms that influence bone activity, and much of the research has been directed towards the study of factors that modulate the bone functions. Bone is a dynamic tissue that provides support for the body against external forces, provides protection to vital internal organs, acts as a lever system to transfer muscular forces, as well as having physiological functions acting as a reservoir of ions and blood cell formation [9]. The requirement of the material used for bone implant is that it presents the biological and mechanical properties of original bone. Human bone is composed of nano-sized organic and mineral phases to form a macrostructure. Proteins present in extracellular matrix of bone are nano-structured comparable to collagen fibrils. Furthermore, calcium phosphate, an important constituent of the bone matrix, is compositionally and structurally nano-structured. Nanostructured materials are unique materials that simulate dimensions of constituent components of bone since they possess particle or grain sizes less than 100 nm [10].

Hydroxyapatite (HA) is the main mineral component of bone (70% of bone composition) [11, 12]. This component has been extensively studied as a material for bone implantation, and its excellent bioactivity and osteoconductivity has been clearly established [10, 13, 14]. From this, efforts have been made to match the material to be implanted with the biological properties of hydroxyapatite and one possibility is to cover with a layer of bioactive material [11, 15].

Currently, in the medical field, there is a clear need for new therapies targeted to provide repair and bone regeneration due to the high incidence of bone defects. Bone defects often arise secondary to trauma, infection, tumor and periprosthetic osteolysis. The deficiencies recognized in bone autografts for the treatment of these conditions led to a large field of research dedicated to the discovery of new bone substitutes [3, 5].

Therefore, the objective was to investigate, *in vivo*, using micro energy-dispersive X-ray fluorescence spectrometry (μ-EDXRF) mapping measurements and scanning electron microscopy-energy dispersive spectroscopy (SEM-EDS) analysis, the biological performance of uncoated and apatite-coated Al_2O_3 implants in rabbits.

MATERIALS AND METHODS

Preparation of ceramic implants for in vivo implantation

The porous Al_2O_3 implants were prepared by gelcasting method [16]. Twelve samples of Al_2O_3 implants were prepared round shaped (4.0 mm of diameter and 2.0 mm high), and half of this samples (n = 6) were apatite-coated by the modified biomimetic method. Three experimental groups were tested: Group C - control, surgery procedure without ceramic implant, Group Ce - uncoated Al_2O_3 implants (n = 6) and Group CeHA - apatite-coated Al_2O_3 implants (n = 6).

Animal care and study protocol

This study was conducted according to the Ethical Principles on Animal Experimentation adopted by the Brazilian College of Animal Experimentation (COBEA) and was approved by the Committee for Ethics in Research of the Faculdade Integral Diferencial - FACID (protocol n. 165/10).

Nine young male adult New Zealand white rabbits (180 days of age, average weight 6 kg) obtained from the FACID bioterium were kept in individual cages, fed a standard laboratory diet, and given tap water ad libitum. The animals were submitted to the anesthesia with ketamine chloride (50 mg/mL) (Dopalen®, Sespo Indústrias e Comércio Ltda, Paulínea-SP, Brazil) and Xylazine (20 mg/mL) (Anasedan®, Sespo Indústrias e Comércio Ltda, Paulínea-SP, Brazil) in the proportion of 1:1 (0.1 ml for each 100 g of animal weight). The surgery procedure was performed on the right tibia of rabbits, and began with the trichotomy and asepsis with topic polvidine (Ceras Johnson® Ltda, Manaus, Amazonas, Brazil) of the site to be incised.

Surgical procedures were common to all animals and consisted of implantation of 2 Al_2O_3 implants in the right tibia of each animal, distant 5 mm apart. The preparation for implantation was performed by a drill-type trephine 4.5 mm and a surgical micro-motor (model AEU-707A, Woodinville, WA, USA) with copious irrigation with saline to undergo a bone defect in elliptical shape with dimensions of 4.5 mm and a depth up to the medullary canal where it has been filled by alumina implant. After the insertion of the implant, the periosteum was repositioned, and suturing was performed up to the skin (#4.0 silk suture, Somerville®, São Gonçalo, RJ, Brazil).

After 30 days [17], the animals were euthanized with an overdose of barbiturates (sodium pentobarbital – 60 mg/kg Tiopentax®, Cristália Produtos Químicos Farmacêuticos, Itapira, SP, Brazil). Next, the tibia of each animal was dissected and removed, sectioned into four segments by a diamond disk (SF 355.504.220, Edenta, São Paulo, SP, Brazil) and each block contained an approximately 4 mm of bone adjacent to the implant. The specimens were labeled and stored in liquid nitrogen.

μ-EDXRF mapping measurements

Semi-quantitative elemental analyses of calcium (Ca) and phosphorus (P) were carried out before and after treatments using an energy-dispersive micro X-ray fluorescence spectrometer μ-EDX 1300 (Shimadzu Corp., Kyoto, Japan), equipped with a rhodium X-ray tube and a Si (Li) detector cooled by liquid nitrogen. The spectrometer was attached to a computer system for data acquisition and processing. The equipment calibration and chemical balance were performed as previously reported [18]. Surface area mappings (n = 18, 20 x 20 points) with steps of 20 μm, 20 s per point, and 50 kV of voltage in the tube were performed in the bone near the surgery defect (Group C) and in the implant-bone interface (Groups Ce and CeHA). The data of Ca and P content were processed by the equipment software (Shimadzu microEDX MP ver. 1.03) after measurements, obtaining thus average values for each component.

SEM-EDS analysis

After treatments, the samples were dehydrated using a graded series of ethanol (30%, 50%, 70%, 95% and 100%) for 10 min at each step. Drying occurred at room temperature after adding a 1:1 solution of hexamethyldisilazane (HMDS), then the samples received a thin layer of gold and were examined using a scanning electron microscope (EVO-MA10, Carl ZeissTM, Oberkochen, Germany) with an acceleration voltage of 20 kV. The SEM images were captured at the magnification of 500x to view the morphology of bone-implant interface. The amounts of Ca and P were measured at three different points by energy dispersive spectroscopy (EDS).

Statistical Analysis

Comparisons among treatments groups were performed using the one-way ANOVA test at a 95% confidence level and the Tukey–Kramer multiple comparisons post-hoc test with GraphPad Prism 5.0 software (GraphPad Software Inc., La Jolla, CA, USA).

RESULTS

μ-EDXRF Mapping

The μ-EDXRF method included qualitative and quantitative microanalysis, as well as element distribution mapping. Table I provides the descriptive statistics for our database with the mean and standard deviations of mineral bone content obtained by X-ray fluorescence of the experimental groups. Statistical comparisons showed higher calcium (Ca) content in specimens of CeHA group than in the Ce ($p < 0.05$) and C ($p < 0.01$) groups. Considering phosphorus content, the CeHA group showed higher phosphorus content than in the C group ($p < 0.01$). The Ca/P ratio of CeHA group was higher than in the C ($p < 0.01$) and Ce ($p < 0.05$) groups.

Table I - Mean and standard deviation of calcium and phosphorus weight percentages (%) and Ca/P molar ratios obtained by x-ray fluorescence of experimental groups: control group (C), uncoated apatite Al_2O_3 ceramic (Ce), and apatite-coated Al_2O_3 ceramic (CeHA). Statistical comparisons were performed by ANOVA and Tukey test.
[Tabela I - Média e desvio padrão das porcentagens em peso (%) de cálcio e fósforo e da relação molar Ca/P obtidos por fluorescência de raios X dos grupos experimentais: grupo controle (C), cerâmica de Al_2O_3 sem recobrimento de apatita (Ce) e cerâmica de Al_2O_3 com recobrimento de apatita (CeHA). As comparações estatísticas foram realizadas pelos testes ANOVA e de Tukey.]

Groups	Ca	P	Ca/P
	Mean (SD)	Mean (SD)	Mean (SD)
C	5.86 (1.62)	4.05 (1.22)	1.459 (0.12)
Ce	10.18 (3.83)	6.92 (1.94)	1.443 (0.205)
CeHa	16.55 (2.89)[a,b]	9.83 (2.38)[a]	1.794 (0.07)[a,b]

[a] *(statistical difference with the group C, $p < 0.01$);*
[b] *(statistical difference with the group Ce, $p < 0.05$).*

In the distribution map provided, relative concentrations are indicated by a black and white scale: black represents minimum concentrations values and white denotes maximum concentration values of the respective pure component spectrum (Fig. 1). The images obtained by surface area mapping showed that the bone implant with an apatite-coated Al_2O_3 ceramic (group CeHA) resulted in greater mineralization with higher calcium and phosphorus content (white color) throughout the surface than in the other groups (C and Ce) (Fig. 1).

SEM-EDS analysis

The SEM micrograph of the Al_2O_3 implant is shown in Fig. 2. It was possible to note a homogeneous macrostructure with roughly surface. Fig. 3 shows the SEM micrographs of the experimental groups. In the micrograph of the bone surface without ceramic implant (Fig. 3a) it can be noted a thin layer of bone tissue and a large area without bone filling. In the group Ce, it could be observed a heterogeneous area with the presence of implanted material relief (Fig. 3b) and, in the group CeHA, a more homogeneous area was found than in the other treatments with an aspect of compact bone and without the relief of the implanted material (Fig. 3c).

Elemental analysis with EDS spectroscopy showed higher calcium percentages in CeHA group than in groups C and Ce ($p < 0.001$) (Table II) and without significance from bone tissue ($p > 0.05$). Specimens of group Ce also showed higher Ca content than in group C ($p < 0.01$) and lower Ca content than in normal bone tissue ($p < 0.01$).

Higher phosphorus content was found in groups CeHA and Ce than in group C ($p < 0.001$) and no statistical differences were found between groups CeHA and Ce ($p > 0.05$). Also,

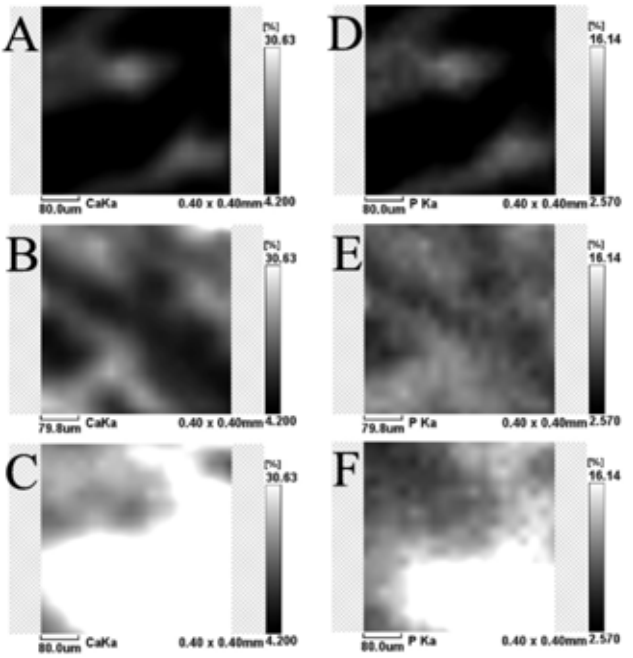

Figure 1: μ-EDXRF elemental distribution images of a representative area (0.20×0.20 mm) showing the calcium (A-C) and phosphorus (D-F) distribution in the bone-implant interface considering the experimental groups: (A, D) control – without ceramic implant; (B, E) uncoated apatite Al_2O_3 ceramic; (C, F) apatite-coated Al_2O_3 ceramic. The gradient in the intensity of the black and white scale indicates variation in calcium and phosphorus component content in percentage, thus a high content shows as light gray and white colors and sites with low content shows as black color. The apatite-coated Al_2O_3 ceramic implant in the bone resulted in greater mineralization in bone around the implant with higher calcium and phosphorus content (white colors) throughout the surface than in the other groups.

[Figura 1: Imagens de distribuição elemental por μ-EDXRF de área representativa (0,20x0,20 mm) mostrando a distribuição de cálcio (A-C) e fósforo (D-F) na interface implante-osso considerando os grupos experimentais: (A, D) controle – sem o implante cerâmico; (B, E) cerâmica de Al_2O_3 sem recobrimento; (C, F) cerâmica de Al_2O_3 recoberta com apatita. O gradiente da intensidade da escala de preto e branco indica a variação no teor de cálcio e de fósforo em percentagem do componente, assim, um elevado teor mostra como as cinza claro e branco e locais com teor baixo aparecem com a cor preta. O implante de cerâmica de Al_2O_3 recoberta com apatita no osso resultou em maior mineralização ao redor do implante com maior teor de cálcio e de fósforo (cores brancas) em toda a superfície do que nos outros grupos].

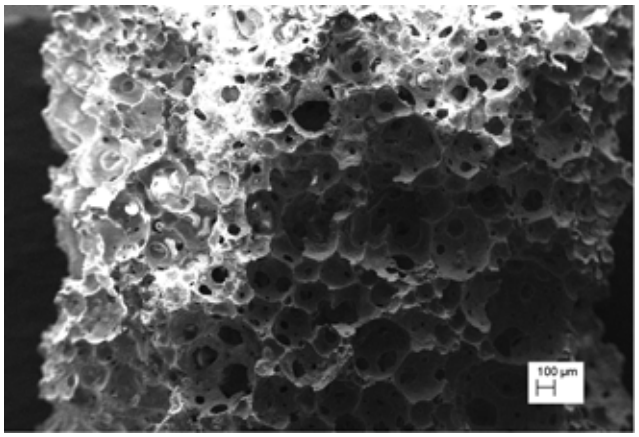

Figure 2: SEM micrograph of the uncoated apatite Al_2O_3 ceramic showing the roughly spherical porous surface which could provide an optimal stratum for bone tissue ingrowth.

[Figura 2: Micrografia obtida por microscopia eletrônica de varredura da cerâmica de Al_2O_3 sem recobrimento, mostrando a superfície rugosa com poros esféricos, que podem proporcionar um estrato ideal para o crescimento do tecido ósseo.]

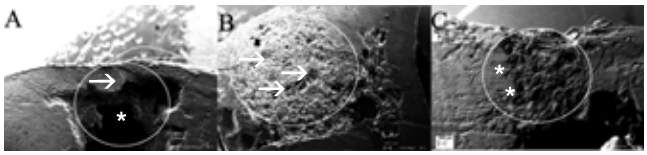

Figure 3: SEM micrographs of the bone-ceramic implant surface after 30 days of surgery (500x): (a) Control group (C) – there is a large unfilled area (*) with a thin layer of bone tissue (arrow); (b) uncoated apatite Al_2O_3 ceramic (Ce) - there is a heterogeneous area (highlight) with the presence of relief (arrow) of implanted material; (c) apatite-coated Al_2O_3 ceramic (CeHA) - it can be noted a more homogeneous area (highlighted) than in the other treatments, where it can be noted an aspect of compact bone and without the relief of the implanted material (*).

[Figura 3: Micrografias obtidas por microscopia eletrônica de varredura da superfície do implante cerâmico com o osso após 30 dias da cirurgia (500x): (a) grupo controle (C) - existe uma grande área não preenchida (*) com uma fina camada de tecido ósseo (seta); (b) cerâmica de Al_2O_3 sem recobrimento (Ce) - existe uma área heterogênea (destaque) com a presença de relevo (seta) do material implantado; (c) cerâmica de Al_2O_3 recoberta com apatita (CeHA) - pode ser notada uma área mais homogênea (destaque) do que nos outros tratamentos, onde pode ser notado um aspecto de osso compacto e sem o relevo do material implantado (*).]

no statistical differences in the phosphorus content were found between bone tissue and groups CeHA and Ce ($p > 0.05$). The Ca/P ratio of CeHA group was higher than in the C ($p < 0.01$) and Ce ($p < 0.05$) groups. The Ca/P ratio of normal bone tissue was higher than in the C ($p < 0.01$) and Ce ($p < 0.05$) groups.

DISCUSSION

Elemental analysis of the bone tissue demonstrated the presence of calcium and phosphorus, pointing to the presence of mineralized bone tissue on the alumina implant surface and in the margins of implant (Figs. 1 and 3). This observation suggests that the homogeneous macrostructure with roughly spherical porous surface of uncoated (Fig. 2) and apatite-coated Al_2O_3 implants could provide an optimal stratum for bone tissue ingrowth. Furthermore, SEM analysis showed that a new bone matrix had developed over the implant surface (Fig. 3).

The μ-EDXRF mappings of the bone-implant interface, and SEM-EDS analysis of surface showed significant calcium and phosphorus in bone indicating the ingrowth of bone around the uncoated and apatite-coated Al_2O_3 implants

Table II - Mean and standard deviation percentages of calcium and phosphorus and Ca/P ratios obtained by EDS spectroscopy analysis (point measurements) of experimental groups: control group (C), uncoated apatite Al_2O_3 ceramic (Ce), and apatite-coated Al_2O_3 ceramic (CeHA). Statistical comparisons were performed by ANOVA and Tukey test.
[Tabela II - Média e desvio padrão das porcentagens em peso (%) de cálcio e fósforo e da relação molar Ca/P obtidos pela análise por espectroscopia por dispersão de energia (análises por pontos) dos grupos experimentais: grupo controle (C), cerâmica de Al_2O_3 sem recobrimento de apatita (Ce) e cerâmica de Al_2O_3 com recobrimento de apatita (CeHA). As comparações estatísticas foram realizadas pelos testes ANOVA e de Tukey.]

Groups	Ca	P	Ca/P
	Mean (SD)	Mean (SD)	Mean (SD)
C	6.79 (1.48)	4.39 (0.59)	1.53 (0.16)
Ce	12.28 (1.26)[a]	7.95 (0.67)[c]	1.54 (0.05)
CeHa	18.06 (2.87)[c,d]	9.76 (1.88)[c]	1.86 (0.16)[a,b]
Bone	16.99 (1.60)[c,d]	9.45 (1.06)[c]	1.79 (0.04)[a,b]

[a](statistical difference with the group C, $p < 0.01$); [b](statistical difference with the group Ce, $p < 0.05$).
[c](statistical difference with the group C, $p < 0.001$); [d](statistical difference with the group Ce, $p < 0.01$).

(Tables I and II, Figs. 1 and 3).

The findings of the present study are consistent with reports in the literature in which elemental analysis by SEM-EDS revealed the interaction of anorganic bovine bone with human bone [19] and bone attached to the xenografts [20]. The present findings also corroborate with previous studies of bone-implant interaction [13, 15]. Su et al. [13], characterized by SEM and histological analysis the surface of bone-implanted porous scaffold of mesoporous bioglass/polyamide composite (m-BPC), after 4 weeks of implanted in the rabbit thighbone, and found that the porosity of the implant served as a scaffold for bone growth. The m-BPC scaffolds also exhibited excellent biocompatibility and osteoconductivity, and more effective osteogenesis than the polyamide scaffolds *in vivo*. Shen et al. [15] studied by histology the bone integration at the tendon-bone interface guided by calcium phosphate ceramics, indicating that it acts as a substrate for bone growth.

Fig. 2 shows SEM images of the obtained scaffolds. From the presented images, it can be seen that composite framework constitutes a macroporous structure with interconnected channels. The osseointegration and the long-term performance of the implanted material are determined by the cellular response of the material on contact with a biological environment and the surface morphology of the implant interferes in this mechanism [21]. Implants with a sponge-like topography effectively interpose on a protein and cellular adhesion, various cell movements and phagocytosis including gene expression [22].

The μ-EDXRF mappings of the bone-implant interface done in the present study and SEM images of the surface morphology showed greater bone formation around the uncoated and apatite-coated Al_2O_3 implants (Table I and II). The ceramic behaved as a bioactive surface, because it had a porous architecture associated with the hydroxyapatite that provided a biological adhesion and proliferation of cells in a bone defect [10, 12]. This increased bone ingrowth observed in μ-EDXRF mappings (higher calcium and phosphorus levels in group CeHA, Fig. 1) and SEM images (Fig. 3C) may be due to stand of the blood clot by the ceramic, which reorganized mesenchymal cells, inducing the fibroblasts and osteoblasts growth and with osteoneogenesis induced by hydroxyapatite [11].

The μ-EDXRF analysis proved adequate to analyze the changes that occurred in osseointegration. The sample preparation is quite simple, since it does not require a specific procedure and or dehydration. Measurements can be performed under normal atmospheric conditions, without the need for high vacuum and are non-destructive (the same samples can be used for multiple analyzes). Our results are in agreement with previous studies. Lindgren et al. [23] and Ramírez-Fernández et al. [20] used the SEM-EDS technique to characterize and quantify the levels of Ca and P in osseointegration of synthetic implants and porcine xenografts in maxillary sinuses and found that the implants were gradually substituted by calcium-deficient hydroxyapatite over the healing period and that newly formed bone had become closely attached to the xenografts (verified by the gradual diffusion of calcium ions at the interface).

CONCLUSION

SEM-EDS revealed that apatite-coated Al_2O_3 implants induced significant bone ingrowths than the control and uncoated implants. EDX analysis monitored the bone formation next to the implants with a significant mineralization (Ca and P content) in the newly forming bone at the bone-implant interface. The biomaterial proved to be biocompatible and osteoconductive when used as a bone implant.

ACKNOWLEDGMENTS

The authors are grateful to Fundação de Amparo a Pesquisa do Estado de S. Paulo, FAPESP (Procs. 05/50811-

9 and 2011/17877-7) and UNIVAP for financial support. The authors thank Prof. Dr. E. S. Trichês (Science and Technology Institute, Federal University of S. Paulo, SP, Brazil) for providing the uncoated and apatite-coated Al_2O_3 foams for biological tests.

REFERENCES

[1] F. Matassi, L. Nistri, D. Chicon Paez, M. Innocenti, Clin. Cases Miner. Bone Metab. **8**, 1 (2011) 21-24.
[2] A. Abarrategi, C. Moreno-Vicente, F. J. Martínez-Vázquez, A. Civantos, V. Ramos, J. V. Sanz-Casado, R. Martnez-Corriá, F. H. Perera, F. Mulero, P. Miranda, J. L. López-Lacomba, PLoS ONE 7, 3 (2012) e34117. doi:10.1371/journal.pone.0034117.
[3] L. Yang, M. Y. Hedhammar, T. Blom, K. Leifer, J. Johansson, P. Habibovic, C. A. V. Blitterswijk, Biomed. Mater. **5** (2010) 1-10.
[4] C. Sever, F. Uygur, Y. Kulahci, G. T. Kose, M. Urhan, Z. Kucukodaci, G. Uzun, O. Lu, T. Cayci, Acta Orthop. Traumatol. Turc. **44**, 5 (2010) 403-409.
[5] A. Nauth, E. H. Schemitsch, Indian J. Orthop. **46**, 1 (2012) 19-21.
[6] S. J. Stephan, S. S. Tholpady, B. S. Brian Gross, C. E. Petrie-Aronin, E. A. Botchway, L. S. Nair, R. C. Ogle, S. S. Park, Laryngoscope **120**, 5 (2010) 895-901.
[7] F. A. Macedo, E. H. M. Nunes, W. L. Vasconcelos, R. A. Santos, R. D. Sinisterra, M. E. Cortes, Cerâmica **58**, 348 (2012) 481-488.
[8] J. K. M. F. Daguano, C. Santos, S. O. Rogero, Matéria **12**, 1 (2007) 134-139.
[9] S. A. Lacerda, R. I. Matuoka, R. M. Macedo, S. O. Petenusci, A. A. Campos, L. G. Brentegani, Braz. Dent. J. **21**, 3 (2010) 199-204.
[10] H. Pei, J. L. Wei-Ping, Z. Chang-li, Z. Xiao-nong, J. Yao, Chin. Med. J. **124**, 2 (2011) 273-279.
[11] M. J. Lee, S. K. Sohn, K. T. Kim, C. H. Kim, H. B. Ahn, M. S. Rho, M. H. Jeong, S. K. Sun, Clin. Orthop. Surg. **2**, 2 (2010) 90-97.
[12] O. Zakaria, M. Madi, S. Kasugai, J. Tissue Eng. **3**, 1 (2012) 1-10.
[13] J. Su, L. Cao, B. Yu, S. Song, X. Liu, Z. Wang, M. Li,. Int. J. Nanomedicine **7** (2012) 2547-2555.
[14] G. J. E. Poinern, R. Brundavanam, X. T. Le, S. Djordjevic, M. Prokic, D. Fawcett, Int. J. Nanomedicine **6** (2011) 2083-2095.
[15] H. Shen, G. Qiao, H. Cao, Y. Jiang, Int. Orthop. **34**, 6 (2010) 917-924.
[16] E. de Sousa, F. S. Ortega, V. C. Pandolfelli, Cerâmica **55**, 334 (2009) 151-156.
[17] A. L. Pinheiro, M. E. Gerbi, E. A. Ponzi, L. M. Ramalho, A. M. Marques, C. M. Carvalho, R. C. Santos, P. C. Oliveira, M. Noia, Photomed. Laser Surg. **26**, 2 (2008) 167-174.
[18] L. E. S. Soares, A. M. do Espírito Santo, A. Brugnera Júnior, F. A. A. Zanin, A. A. Martin, J. Biomed. Opt. **14**, 2 (2009) 24002-1-24002-7.
[19] T. Traini, M. Degidi, R. Sammons, P. Stanley, A. Piattelli, J Periodontol. **79**, 7 (2008) 1232-1240.
[20] M. P. Ramírez-Fernández, J. L. Calvo-Guirado, J. E. Maté-Sánchez Del Val, R. A. Delgado-Ruiz, B. Negri C. Barona-Dorado, Clin. Oral Implants Res. **24**, 5 (2013) 523-530.
[21] Ł. John, M. Bałtrukiewicz, P. Sobota, R. Brykner, Ł. Cwynar-Zając, P. Dzięgiel, Mater. Sci. Eng. C. **32**, 7 (2012) 1849-1858.
[22] C. Giordano, F. Causa, L. D. Silvio, L. Ambrosio, J. Mater. Sci. - Mater. Med. **18**, 4 (2007) 653-660.
[23] C. Lindgren, M. Hallman, L. Sennerby, R. Sammons, Clin. Oral Implants Res. **21**, 9 (2010) 924-930.
(Rec. 11/04/2013, Ac. 25/05/2013)